Malaysian Journal of Chemistry, 2022, Vol. 24(4), 10-18
(Special Issue: *8th International Conference for Young Chemists (ICYC) 2022*)

Synthesis and Development of EMT-Type Zeolite-Mediated Silver Nanoparticles as Antibacterial and Antifungal Agent

Nur Farhanah Binti Mohd Amin[1], Phaik Ching Ang[1], Eng Poh Ng[1], Joo Shun Tan[2], Noor Arifah Binti Ahmad Che Hamat[1] and Pandian Bothi Raja[1*]
[1]School of Chemical Sciences, Universiti Sains Malaysia, 11800 Penang, Malaysia
[2]School of Industrial Technology, Universiti Sains Malaysia, 11800 Penang, Malaysia
*Corresponding author (email: bothiraja@usm.my)

The growth of bacterial resistance towards antibiotics is causing the demand for a new alternative to antibiotics. By incorporating silver in zeolite, the release behaviour of silver can be controlled and antibacterial efficiency can be enhanced. In this study, EMT-type zeolite silver nanoparticles (AgNPs) are synthesized. The size and morphology of synthesized EMT-type zeolite AgNPs were further characterized using Ultraviolet-Visible spectroscopy (UV-Vis), Fourier Transform-Infrared Spectroscopy (FT-IR), Transmission Electron Microscopy (TEM) and Scanning Emission Microscopy coupled with Energy Dispersive X-Ray Spectroscopy (SEM-EDX). The size of the silver particles was found within 10.4 to 68.0 nm with a spherical shape and the peak was shown at 301 nm in UV spectrum. The antibacterial and antifungal activity of the synthesized EMT-type zeolite AgNPs was investigated against Gram-positive bacteria (*Staphylococcus aureus*), Gram-negative bacteria (*Escherichia coli*), and fungi (yeast) by agar diffusion method. The inhibition zone on *S.aureus* (19 mm) was larger than *E.coli* (15 mm). Synthesized AgNPs enhanced the antifungal activities on yeast from inhibition zone of 22 mm to 57 mm.

Key words: Nanotechnology; EMT-type zeolite; silver nanoparticles; antibacterial agent; antifungal agent; support material

Received: September 2022; Accepted: November 2022

One of the arising and well-known developing technologies in recent years is nanotechnology, which deals with components with nanoscale dimensions between 1-100 nm [1]. Especially, nanoparticles that have a small dimension give a high surface-to-volume ratio and provide excellent optical, physical, and chemical properties [2]. Nanoparticles exhibit shape and size-dependent features that can be customized widely[3]. Different nanoparticles are utilized for a variety of applications such as molecular tagging, textile industries, quantum computers, bio-imaging, energy, quantum lasers, environment, and anti-microbial coatings [3].

Among many types of metal nanoparticles, noble metal nanoparticles, i.e., Au, Ru, Pt, Rh, Pd, Os and Ir, especially silver nanoparticles (AgNPs), have been widely studied and become a notable material among researchers [4]. Because of the specific properties that AgNPs possess, they have found widespread use in a variety of applications, including medical diagnostics, antibacterial treatments, conductive materials, and optical devices [1,5,6]. Due to their large surface area and thermal stability, AgNPs can provide a prolonged and controlled release of silver ions (Ag^+) effectively for their antibacterial durability unlike bulk metals [7,8]. Ag^+ exhibit high bactericidal efficiency by the action of engagement with the bacterial inner cell membrane and the reactive oxygen species (ROS) discharge [9]. AgNPs demonstrate extraordinary antimicrobial properties due to their high surface-to-volume ratio and the ability to continuously release Ag+, which is regarding the microbes' death mechanism [10]. The permeability of the cell membrane was changed by the neutralization of the bacterial surface charge, which eventually resulted in cell death after anchoring AgNPs to the surface of the cell [10].

The drawbacks of AgNPs are the particles are thermodynamically unstable and aggregate easily. Hence, the particle growth activity must be controlled, by inorganic capping compounds, metal salts or organic ligands able to generate core-shell-type particle morphologies. In this context, the combination of porous materials (EMT-zeolites) has the potential to serve as a good supporting material in nanotechnology [11–13]. The smaller size of the organized voids and canals of the zeolite inhibits the formation of clusters and nanoparticles thus controlling their size at nanosized ranges [14]. Zeolites offer a one-of-a-kind support structure from the point of view of the storage and release of silver due to its substantial surface area, uniform micro-porous structure, strong acidity and high capacity for ion exchange [15]. Ion exchange can take place in zeolites with an aluminosilicate framework owing to the framework's ability to hold variable amounts of

†Paper presented at the 8th International Conference for Young Chemists (ICYC) 2022

Ag^+. Additionally, AgNPs can be formed both within and on the surface of zeolite, using the zeolite itself as an anchoring agent [16].Due to the superior 3D topological structure of EMT-type zeolite and larger cavities as well as a greater number of windows, many studies have focused on EMT-type zeolite compared to the FAU-type zeolite [17,18].

Bacterial infections are the primary source of human health issues. There are two main categories of bacteria, i.e., Gram-positive and Gram-negative bacteria. They are differed in the molecular components and architecture of the outermost cell wall, particularly in terms of disposition, cell wall structure and membrane [19]. In bacteria, it creates a protective barrier and mesh-like structure that builds up the cell wall (peptidoglycan). Gram-positive bacteria have a notably thicker peptidoglycan layer (20-30 nm) compared to Gram-negative bacteria (6-7 nm) [20]. The cell's responses to external stimuli including heat, UV light, and antibiotics are affected by these differences in the cell membrane [21]. Antibacterial agents could hinder bacterial growth, resulting in the failure of crucial cellular activities and ultimate cell death. The use of synthetic antibiotics also has its downside. If the human body intakes the antibiotic for frequent time, the body can develop a resistance to antibiotics and causing the antibiotic to be less effective. Moreover, the growing resistance of pathogenic bacterial strains makes the infections harder to treat with antibiotics. In recent developments, combining antibiotics with metal nano-particles could make the antibiotics more effective against pathogens that are resistant to them. According to Naqvi et al., the antibacterial activity of imipenem, gentamycin, vancomycin and ciprofloxacin with impregnated AgNPs has shown a significant increase toward the drug-resistant pathogens [22]. Thus, nano-medicine can be seen as a new light to create a novel treatment for bacterial infections.

This study emphasized the supported AgNPs on EMT-type zeolite under laboratory control. The antibacterial effect of silver nanoparticles supported on EMT-type zeolite synthesized was investigated on Gram-positive bacteria (*Staphylococcus. aureus*), Gram-negative bacteria (*Escherichia. Coli)*, and fungi (commercial yeast).

EXPERIMENTAL SECTION

1. Materials

Sodium hydroxide (NaOH, Prolabo), sodium alumiate ($NaAlO_2$, 53%, 42.5% Na_2O, Sigma Aldrich) and collected rice husk ash were used to synthesize EMT-type zeolite. The synthesized EMT-type zeolite and silver nitrate ($AgNO_3$) were used to synthesize the AgNPs supported on EMT-type zeolite. Silver nitrate ($AgNO_3$) was supplied by R&M chemicals that are used as silver ions precursors. Filtered water was used as the solvent throughout the reaction. The bacteria used to represent negative and positive gram bacteria is *Escherichia. coli (E. coli) and Staphylococcus. aureus (S. aureus)* respectively. Both bacteria were obtained from School of Industrial Technology, USM. The yeast used is a commercial instant yeast brand Mauri-Pan bought at a local hypermarket in Penang, Malaysia.

2. Synthesis of EMT-type Zeolite

The EMT-type zeolite was prepared according to the previous study by Ng et al. [23]. Firstly, sodium hydroxide, NaOH (25.58 g, Prolabo, 99%) and rice husk ash (RHA) (6.00 g) were dissolved in distilled water (31.16 g) for 2 h at 100℃ to prepare for solution A. Next, NaOH (1.00 g, Prolabo, 99%) and sodium aluminate (3.73 g, $NaAlO_2$, 53%, 42.5% Na_2O Sigma-Aldrich) were dissolved in distilled water (46.74 g) to prepare solution B. While being vigorously stirred, solution B was gradually added into solution A to produce a mixture with gel consistency having a chemical composition of SiO_2:Al_2O_3:Na_2O:H_2O at the ratio of 5:1:18:217. The gel mixture was stirred continuously for 10 min and then undergo crystallization for 28 h at 28 ℃. At various intervals during the crystallization process, the solids were extracted using high-speed centrifugation (20,000 rpm, 60 min), and then re-dispersed in double-distilled water. This process was done repetitively until the final pH of colloidal suspensions was pH 7.5.

3. Synthesis of EMT-type Zeolite-mediated AgNPs

EMT-type zeolite and $AgNO_3$ was prepared in 1000 ppm with distilled water in 100 mL volumetric flask respectively and 50 ml of each solution was mixed and continually stirred using a magnetic stirrer hotplate for 48 h. The synthesized EMT-type zeolite AgNPs was centrifuged using Tabletop Centrifuge Model-4000 (Kubota) at 3500 rpm for 15 min to separate the excess EMT-type zeolite AgNPs brown sediment from the suspension. The sample was kept in the fridge for further characterization.

4. Characterization of Synthesized EMT-type Zeolite AgNPs

The AgNPs were characterized by the following analysis to study the structure, size, morphology, and characteristic of the synthesized EMT-type zeolite AgNPs.

4.1. Ultraviolet-Visible (UV-Vis) Spectroscopy

The characteristic peak of AgNPs was confirmed using UV-Vis spectrophotometer (Shimadzu UV-2600) between 200-700 nm. The reading was recorded at every hour within 2 days of continuous stirring. All UV-Vis analysis was done at School of Chemical Sciences, USM.

4.2. Fourier Transform Infrared Spectroscopy (FTIR)

FT-IR spectroscopy (Perkin Elmer FT-ATR Spectrometer) was used to characterize the synthesized EMT-type Zeolite AgNPs before and after. The FT-IR spectra were recorded in the range of 400-4000 cm^{-1}.

4.3. Transmission Electron Microscopy (TEM)

The size and morphology of synthesized EMT-type zeolite AgNPs were investigated by TEM using TEM Carl Zeiss Libra ® 120 (School of Biological Sciences, USM). A carbon-coated grid was put on the filter paper. From the AgNPs colloid, 1-2 drops of the sample were dropped onto the grid and left to dry naturally. Then, the sample was analysed by TEM machine. The particle size distribution was measured from selected 45 particles in TEM images.

4.4. Scanning Emission Microscopy with Energy Dispersive X-Ray Spectroscopy (SEM-EDX)

The structure and the elemental composition of the synthesized EMT-type zeolite AgNPs was determined by SEM-EDX using Carl Zeiss Leo Supra 50 VP Field Emission equipped with Oxford INCA-X energy dispersive microanalysis system (School of Biological Sciences, USM). The synthesized sample was mounted on the aluminium stubs using a carbon sticky tape. From the AgNPs colloid, 1 – 2 drops of sample were dropped on the sticky tape and left to dry for 3-4 h. Once the sample dried and mounted on the stubs, the sample was coated with gold coating to enhance the clarity of the sample.

5. Antibacterial and Antifungal Test

The antibacterial and antifungal effect of synthesized EMT-type zeolite AgNPs was investigated using the agar well diffusion method against *E. coli*, *S. aureus* and yeast. *E. coli* and *S. aureus* bacteria were first sub-cultured overnight. The preparation for subculturing the bacteria was done by adding 1 mL of stock bacteria with 9 mL of BHI (Brain Heart Infusion) broth and then kept in the fridge overnight. For the yeast preparation, the instant yeast was revived with autoclave water by adding 1 g of the instant yeast to 10 mL of autoclave water and left for 30 min for it to revive.

Six agar plates were prepared for antibacterial testing. Two plates for each bacterium and yeast were prepared. One was tested on EMT-type zeolite, and one was tested on the synthesized EMT-type zeolite AgNPs. Each plate was spread with 100 µL respective bacteria and yeast evenly. Three wells were formed by punching the medium using a sterilized Pasteur pipette. Then, 100 µL of zeolite was inserted in each hole and then the agar plate was sealed and left for incubation at controlled temperature overnight. Same steps were repeated using synthesized EMT-type zeolite AgNPs. The plates containing *E. coli* and *S. aureus* were incubated at 37 ℃ for 24 h while the plates containing yeast were incubated at 25 ℃ for 24 h. The inhibition zone was observed after 24 h. The inhibition zone was measured in millimetres.

RESULT AND DISCUSSION

1. UV-Vis Spectroscopy Analysis

The colour change was observed after 6 h of stirring from a clear solution to light shady brown colour as shown in Figure 1. The colour appearance was due to the changes of Ag^+ ion to AgNPs. Hence, this is considered as the first evidence for the synthesis of AgNPs. The appearance of a strong UV-Vis spectrophotometric peak between 280 and 320 nm confirmed the formation of AgNPs (Figure 2a) [24]. The maximum absorbance for the transition of Ag^+ ions to AgNPs started after 6 h of stirring continuously. The peak centered at 301 nm indicates the wavelength of AgNPs formed. However, a decrease in absorbance of AgNPs is observed as the sample was continuously stirred for 48 h (Figure 2a). Aggregation of nano-particles could be the reason for the decrease of UV absorption. According to Pellegrino et al. [25], as the aggregation size of particle increase, the absorption in UV will decrease since the scattering in the visible region increases. Thus, we can assume that the aggregation size of AgNPs is increased as the UV absorption is decreased through 48 h of continuous stirring. According to Hashim et al., the diameter size of AgNPs affects its optical properties [1]. A nano-particle's diameter increases above 40 nm when the surface plasma resonance (SPR) peaks shift towards longer wavelengths (near and above 400 nm), while the SPR peaks show at the shorter wavelengths when the diameter is less than 20 nm. The UV peaks observed in Figure 2b at 280-320 nm indicate that the AgNPs particle size might be in the range of 30-60 nm. Results in TEM and SEM analysis were also in good agreement with UV-Vis results.

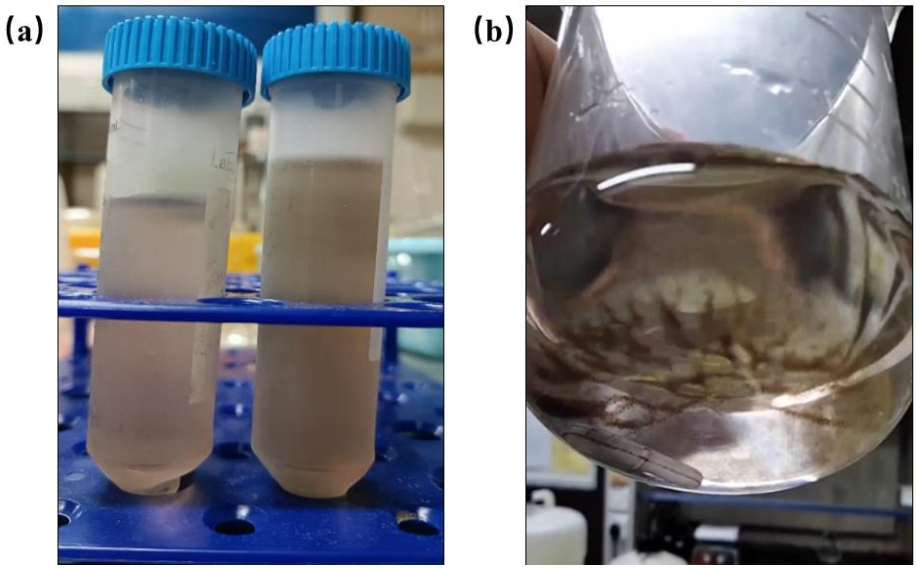

Figure 1. Formation of EMT-type zeolite AgNPs. (a) Colour of EMT-type zeolite AgNPs, (b) Obvious aggregation of AgNPs.

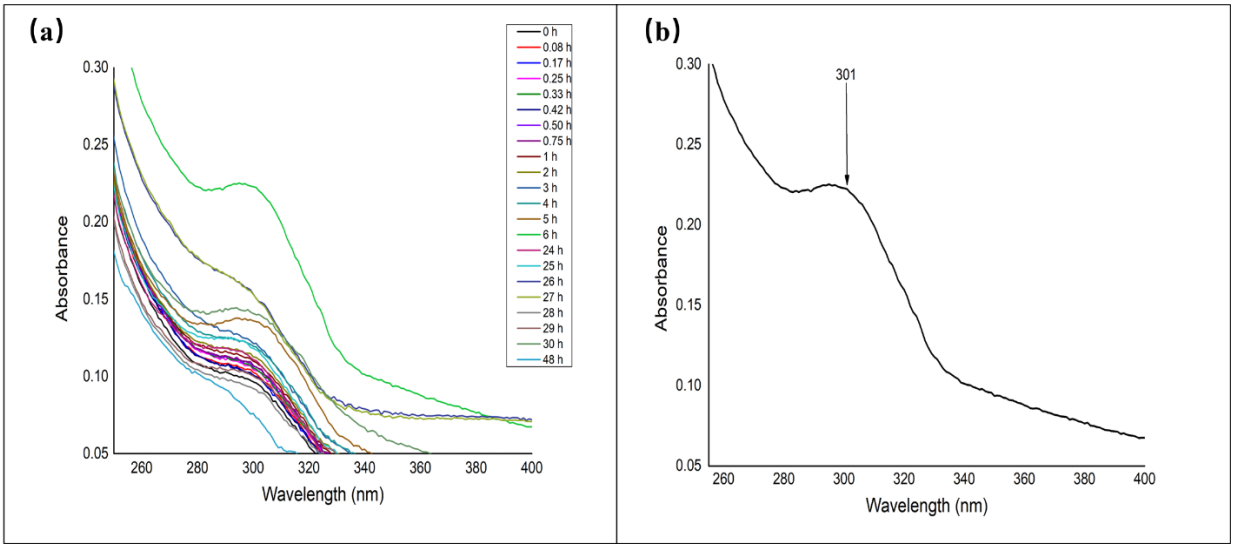

Figure 2. UV-Vis spectra of (a) synthesized EMT-type zeolite AgNPs at different time, (b) synthesized EMT-type zeolite AgNPs after 6 h.

2. FT-IR Spectroscopy Analysis

The FTIR-ATR spectroscopy was used to identify the characteristic peaks of synthesized EMT-type zeolite AgNPs before and after forming. Based on Figure 3, The broad peaks appearance at 3298 cm^{-1} and 1636-1634 cm^{-1} correspond to the hydroxyl groups (-OH) due to the H_2O inter-porous structure of O-H stretching (H-bonding) for H-O-H bending, respectively. The bands at 534-520 cm^{-1} correspond to the Al-O bond and 462-412 cm^{-1} was assigned to the Si-O-Si bending vibration. The presence of van der Waals interactions between -OH groups in the EMT-type zeolite structure associated with H_2O and the partial positive charge on the surface of AgNPs resulted to a broad peak [26]. Furthermore, it was observed that both compounds exhibit almost the same IR spectra but there is slight difference at region 520-400 cm^{-1} which correspond to Al-O bond and Si-O-Si bond. The introduction of Ag into the zeolite might decrease the dipole moment of Al-O bond and Si-O-Si bond and thus shifts the absorption to a lower wave-number. Hence, the absorption peaks for Al-O bond and Si-O-Si bond in EMT-type zeolite AgNPs is at lower wavenumber compared to in EMT-type zeolite only. This shows that incorporation of AgNPs into EMT-type zeolite does cause any structural changes to the EMT-type zeolite frameworks.

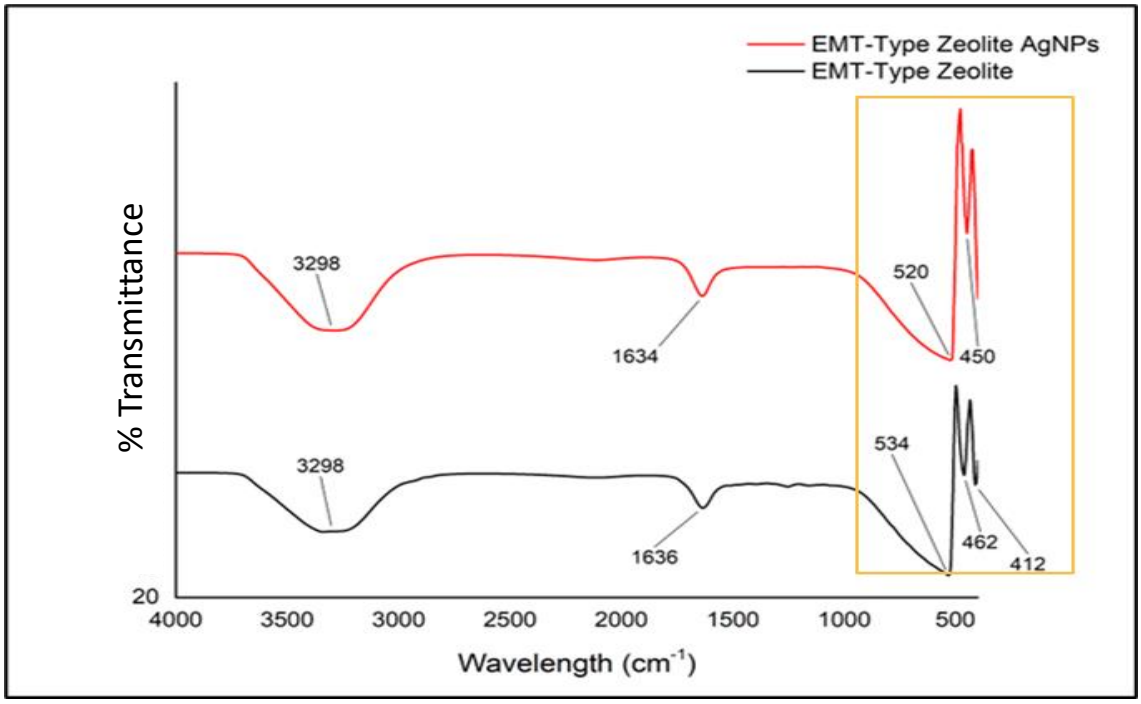

Figure 3. FT-IR spectra of EMT-type zeolite AgNPs (red) and EMT-type zeolite (black).

3. TEM Analysis

The morphology and size of synthesized AgNPs were investigated by TEM analysis. From the TEM images in Figure 4, the distribution of AgNPs in the EMT-type zeolite matrix was observed as the dark contrast spots in the electron micrographs. This confirms that the AgNPs were successfully synthesized and incorporated in EMT-type zeolite. The morphology of AgNPs formed was in a spherical structure. From the data obtained, the range size of the AgNPs is 10.4 to 68.0 nm with an average of 32.8 nm. The size of AgNPs formed was within the size range for nanoparticles which are 1-100 nm. The EMT-type zeolite matrix can control the size distribution of AgNPs into smaller sizes, proving to be a potential reducing and capping agent in nanoparticles synthesis. The distribution of AgNPs is well dispersed within the EMT-type zeolite matrix with few Ag agglomerations. Some huge Ag clusters can be observed in Figure 4 (a) at resolution 8k. The hexagonal framework of EMT-type zeolite also can be observed in the TEM images in Figure 4 (d) at 80k.

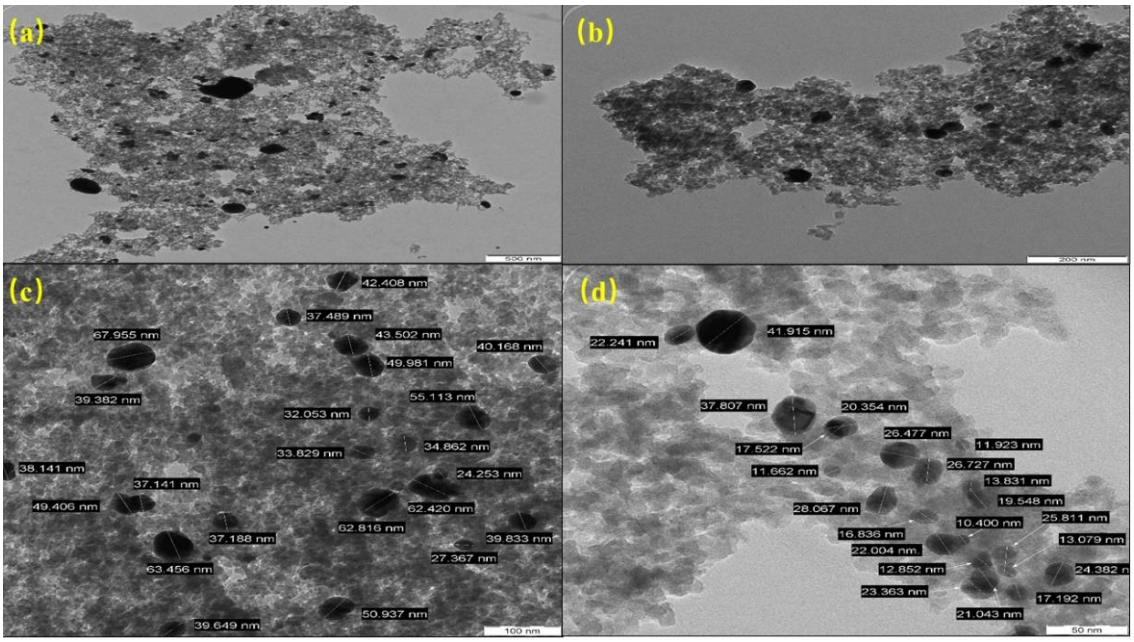

Figure 4. TEM images of EMT-type Zeolite AgNPs at (a) 8k, (b) 25k, (c) 40k and (d) 80k resolution.

4. SEM-EDX Analysis

Based on the SEM micrographs, the synthesized AgNPs can be observed from the white contrast spots. The AgNPs were distributed in the EMT-type zeolite matrix as it was observed that the white spots existed in the hexagonal framework of the EMT-type zeolite. It proved that the Ag^{+} ion is successfully exchanged and then reduced to Ag^{0} inside the EMT-type zeolite channel [27]. In Figure 5 (b), Ag clusters are observed, which indicated that Ag agglomeration also occurs despite the AgNPs being well dispersed within the EMT-type zeolite matrix [28].

The elemental composition of synthesized EMT-type zeolite AgNPs was investigated using EDX spectrum. The EDX analysis showed a strong signal for Ag at approximately 3 keV. This confirms the presence of AgNPs in the synthesized sample. Other minor elements were also detected in the sample, which are Carbon (C), Oxygen (O), Aluminium (Al) and Silicon (Si) atoms. Al, Si and O atoms could be contributed from EMT-type zeolite, while C could be detected because of the carbon tape used in the SEM analysis. The percentage relative composition of each element refers to Table 1.

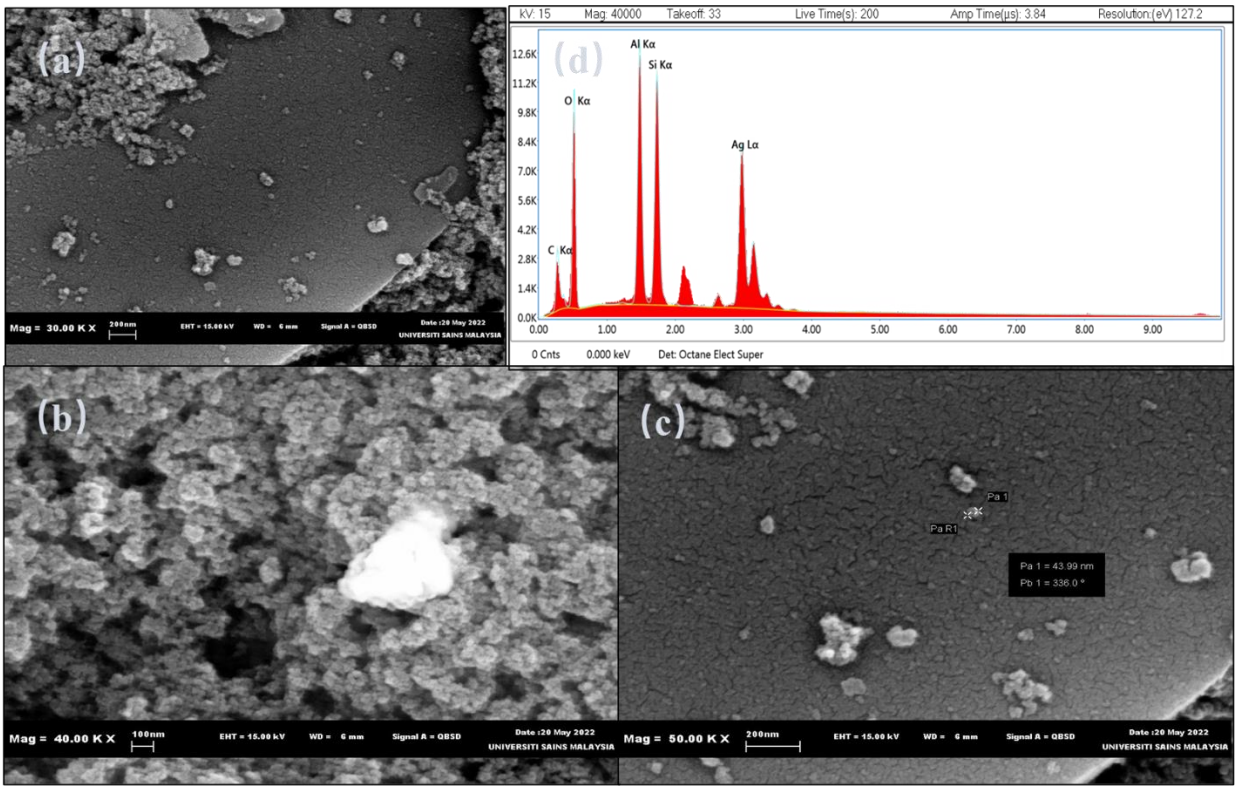

Figure 5. SEM images of EMT-type zeolite AgNPs at (a) 30k, (b) 40k and (c) 50k magnification, and EDX elemental analysis.

Table 1. EDX elemental analysis of synthesized EMT-type zeolite AgNPs.

Element	Weight %	Atomic %	Error %
C	10.75	22.43	10.16
O	28.64	44.86	9.59
Al	14.14	13.13	4.86
Si	13.30	11.87	4.79
Ag	33.18	7.71	2.29

5. Antibacterial and Antifungal Test

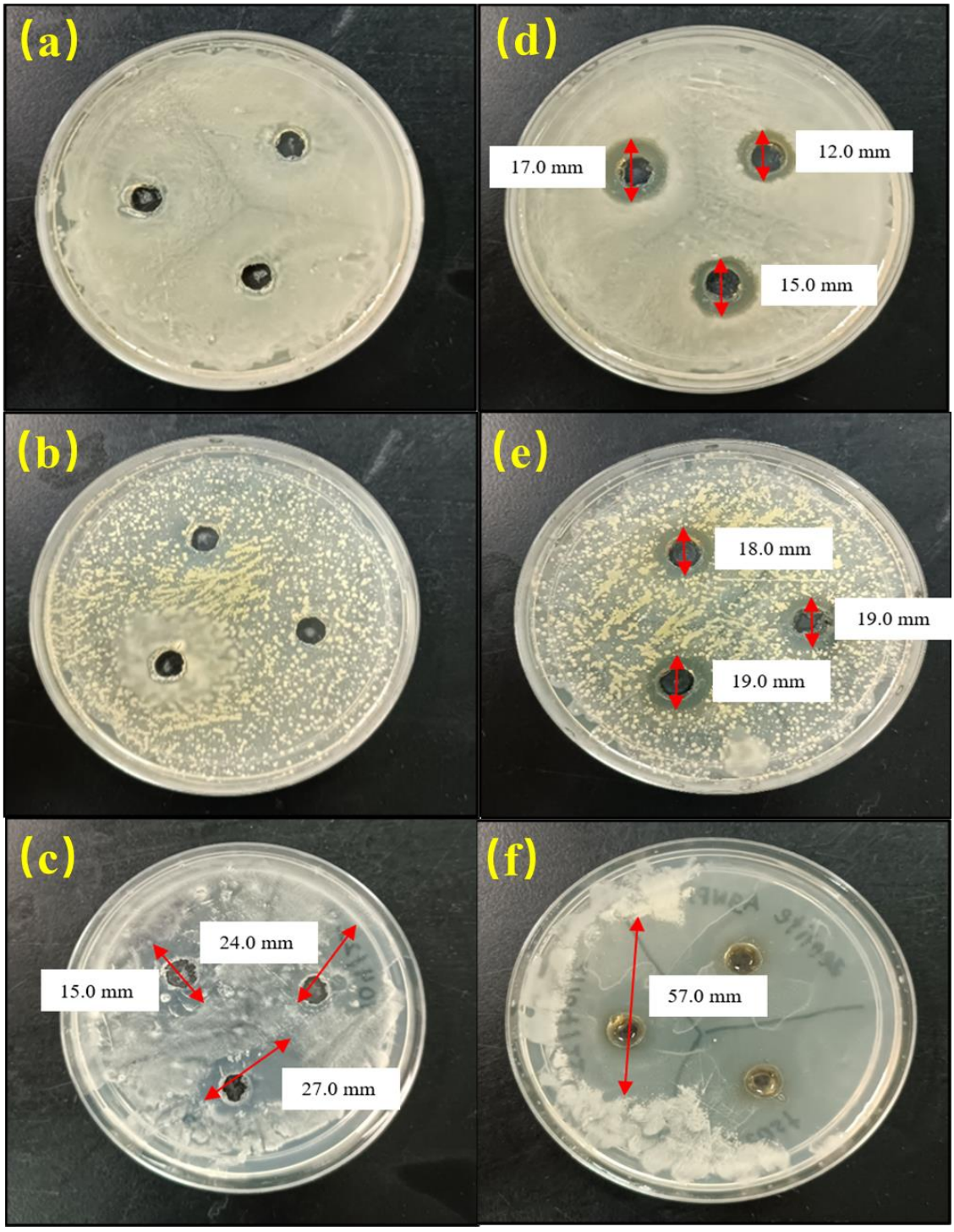

Figure 6. Inhibition zone of (a,b,c) E. Coli, S. aureus, and Yeast with EMT-type zeolite, (d,e,f) E. Coli, S. aureus, and Yeast with EMT-type zeolite AgNPs.

The inhibition zone of the *E. coli*, *S. aureus* and yeast was observed after 24 h of incubation. The EMT-type zeolite does not inhibit the bacterial growth of *E. coli* and *S. aureus* but shows slight antibacterial against yeast. There is no inhibition zone observed for EMT-type zeolite against *E. coli* and *S. aureus.* In contrast, inhibition zone was observed on *E. coli* and *S. aureus* that introduced with EMT-type zeolite AgNPs, where the average inhibition zones are 15.0 mm for *E. coli* and 19.0 mm for *S. aureus*, respectively. A larger inhibition zone (57 mm) was observed when yeast was treated with EMT-type zeolite AgNPs compared to only EMT-type zeolite (19 mm). From the results obtained, EMT-type zeolite AgNPs have successfully inhibit the bacterial growth of *E. coli*, *S. aureus* and yeast. The maximum antibacterial effect of EMT-type zeolite AgNPs was towards yeast, followed by *S. aureus* and *E. coli*.

Table 2. Inhibition of each organism on EMT-type zeolite and EMT-type zeolite AgNPs

Sample	Organisms	Average inhibition zone (mm)
EMT-type zeolite	*E. coli*	None
	S. aureus	None
	Yeast	22.0
EMT-type zeolite AgNPs	*E. coli*	15.0
	S. aureus	19.0
	Yeast	57.0

CONCLUSION

The EMT-type zeolite AgNPs was successfully synthesized and employed for antibacterial activity. The synthesized AgNPs were observed in spherical morphology with diameter ranging from 10.4 to 68.0 nm, and an average of 32.8nm. By using EMT-type zeolite as support for AgNPs synthesis, the size of AgNPs was controlled and well distributed which could be observed from the TEM and SEM analysis. The synthesized EMT-type zeolite AgNPs are able to inhibit the growth of *E. coli, S. aureus* and yeast significantly. From this study, EMT-type zeolite has shown potential as an antibacterial and antifungal agent. In order to evaluate its potential use in treatments for infections, additional research is required.

ACKNOWLEDGEMENT

The authors would like to acknowledge the Ministry of Higher Education Malaysia (MOHE) for funding the Fundamental Research Grant Scheme (FRGS) code: FRGS/1/2021/ STG05/USM/02/4.

REFERENCES

1. Hashim, N., Paramasivam, M., Tan, J. S., Kernain, D., Hussin, M. H., Brosse, N., Gambier, F. and Raja, P. B. (2020) Green mode synthesis of silver nanoparticles using Vitis vinifera's tannin and screening its antimicrobial activity/apoptotic potential versus cancer cells. *Materials Today Communications,* **25**, 101511.

2. Song, W. C., Kim, B., Park, S. Y., Park, G. and Oh, J. W. (2022) Biosynthesis of silver and gold nanoparticles using Sargassum horneri extract as catalyst for industrial dye degradation. *Arabian Journal of Chemistry*, **15(9)**, 104056.

3. Dhand, C., Dwivedi, N., Loh, X. J., Jie Ying, A. N., Verma, N. K., Beuerman, R. W., Lakshminarayanan, R., and Ramakrishna, S. (2015). Methods and strategies for the synthesis of diverse nano-particles and their applications: A comprehensive overview. *RSC Advances.* **5 (127)**, 105003–105037.

4. Tan, K. B., Sun, D., Huang, J., Odoom-Wubah, T., and Li, Q. (2021) State of arts on the bio-synthesis of noble metal nanoparticles and their biological application. *Chinese Journal of Chemical Engineering*, **30**, 272–290.

5. Chernousova, S. and Epple, M. (2013) Silver as antibacterial agent: Ion, nanoparticle, and metal. *Angewandte Chemie - International Edition*, **52(6)**, 1636–1653.

6. Lansdown, A. B. G. (2006) Silver in health care: Antimicrobial effects and safety in use. *Current Problems in Dermatology*, **33**, 17–34.

7. Hidayat, M. I., Adlim, M., Maulana, I., Suhartono, S., Hayati, Z. and Bakar, N. H. H. A. (2022) Green synthesis of chitosan-stabilized silver-colloidal nanoparticles immobilized on white-silica-gel beads and the antibacterial activities in a simulated-air-filter. *Arabian Journal of Chemistry.* **15 (2)**, 103596.

8. Falconer, J. L. and Grainger, D. W. (2017). Silver antimicrobial biomaterials. In *Comprehensive Biomaterials II*. Elsevier, United States.

9. Kędziora, A., Speruda, M., Krzyżewska, E., Rybka, J., Łukowiak, A., and Bugla-Płoskońska, G. (2018) Similarities and differences between silver ions and silver in nanoforms as antibacterial agents. *International Journal of Molecular Sciences.* **19(2)**, 444.

10. Yin, I. X., Zhang, J., Zhao, I. S., Mei, M. L., Li, Q. and Chu, C. H. (2020) The antibacterial mechanism of silver nanoparticles and its application in dentistry. *International Journal of Nanomedicine*, **15**, 2555–2562.

11. White, R. J., Luque, R., Budarin, V. L., Clark, J. H. and Macquarrie, D. J. (2009). Supported metal nanoparticles on porous materials. Methods and applications. *Chemical Society Reviews*, **38(2)**, 481–494.

12. Dong, B., Belkhair, S., Zaarour, M., Fisher, L., Verran, J., Tosheva, L., Retoux, R., Gilson, J. P. and Mintova, S. (2014) Silver confined within zeolite EMT nanoparticles: preparation and

antibacterial properties. *Nanoscale*, **6(18)**, 10859–10864.

13. Salim, M. M. and Malek, N. A. N. N. (2017) Review of modified zeolites by surfactant and silver as antibacterial agents. *Journal of Advanced Research in Material Sciences*, **36 (1)**, 1–20.

14. Flores-López, N. S., Castro-Rosas, J., Ramírez-Bon, R., Mendoza-Córdova, A., Larios-Rodríguez, E. and Flores-Acosta, M. (2012) Synthesis and properties of crystalline silver nanoparticles supported in natural zeolite chabazite. *Journal of Molecular Structure*, **1028,** 110–115.

15. Zeng, X., Hu, X., Song, H., Xia, G., Shen, Z. Y., Yu, R. and Moskovits, M. (2021) Microwave synthesis of zeolites and their related applications. *Microporous and Mesoporous Materials*, **323**, 111262.

16. Dutta, P. and Wang, B. (2019) Zeolite-supported silver as antimicrobial agents. *Coordination Chemistry Reviews*, **383**, 1–29.

17 Xia, S., Chen, Y., Xu, H., Lv, D., Yu, J. and Wang, P. (2019) Synthesis EMT-type zeolite by microwave and hydrothermal heating. *Microporous and Mesoporous Materials*, **278**, 54–63.

18. Nearchou, A., Raithby, P. R. and Sartbaeva, A. (2018) Systematic approaches towards template-free synthesis of EMT-type zeolites. *Microporous and Mesoporous Materials*, **255**, 261–270.

19. Tavares, T. D., Antunes, J. C., Padrão, J., Ribeiro, A. I., Zille, A., Amorim, M. T. P., Ferreira, F. and Felgueiras, H. P. (2020) Activity of specialized biomolecules against gram-positive and gram-negative bacteria. *Antibiotics*, **9 (6)**, 314.

20. Yusupov, M., Neyts, E. C., Khalilov, U., Snoeckx, R., Van Duin, A. C. T. and Bogaerts, A. (2012) Atomic-scale simulations of reactive oxygen plasma species interacting with bacterial cell walls. *New Journal of Physics*, **14**, 093043.

21. Mai-Prochnow, A., Clauson, M., Hong, J. and Murphy, A. B. (2016) Gram positive and Gram negative bacteria differ in their sensitivity to cold plasma. *Scientific Reports*, **6**, 38610.

22. Naqvi, S. Z. H., Kiran, U., Ali, M. I., Jamal, A., Hameed, A., Ahmed, S. and Ali, N. (2013) Combined efficacy of biologically synthesized silver nanoparticles and different antibiotics against multidrug-resistant bacteria. *International Journal of Nanomedicine*, **8**, 187–195.

23. Ng, E. P., Awala, H., Tan, K. H., Adam, F., Retoux, R. and Mintova, S. (2015) EMT-type zeolite nanocrystals synthesized from rice husk. *Microporous and Mesoporous Materials*, **204**, 204–209.

24. Gaddala, B. and Nataru, S. (2015). Synthesis, characterization and evaluation of silver nanoparticles through leaves of Abrus precatorius L.: An important medicinal plant. *Applied Nanoscience*, **5 (1)**, 99–104.

25. Pellegrino, F., Pellutiè, L., Sordello, F., Minero, C., Ortel, E., Hodoroaba, V. D. and Maurino, V. (2017) Influence of agglomeration and aggregation on the photocatalytic activity of TiO2 nanoparticles. *Applied Catalysis B: Environmental*, **216**, 80–87.

26. Shameli, K., Ahmad, M. Bin, Zargar, M., Yunus, W. M. Z. W. and Ibrahim, N. A. (2011) Fabrication of silver nanoparticles doped in the zeolite framework and antibacterial activity. *International Journal of Nanomedicine*, **6**, 331–341.

27. Li, W., Qi, M., Sun, X., Chi, M., Wan, Y., Zheng, X., Li, C., Wang, L. and Dong, B. (2020) Novel dental adhesive containing silver exchanged EMT zeolites against cariogenic biofilms to combat dental caries. *Microporous and Mesoporous Materials*, **299**, 110113.

28. Chouhan, S. and Guleria, S. (2020) Green synthesis of AgNPs using Cannabis sativa leaf extract: Characterization, antibacterial, anti-yeast and α-amylase inhibitory activity. *Matrials Science of Energy Technologies.* **3**, 536–544.